Karim Khayati[1]
Dr.
Department of Mechanical Engineering,
Royal Military College,
15 Valour Drive,
PO Box 17000, Station Forces,
Kingston, Ontario, K7K 7B4, Canada
e-mail: karim.khayati@rmc.ca

Pascal Bigras
Professor
Department of Automated Manufacturing Engineering,
École de Technologie Supérieure,
University of Quebec,
1100 Notre-Dame West Street,
Montreal, Quebec, H3C 1K3, Canada
e-mail: pascal.bigras@etsmtl.ca

Louis-A. Dessaint
Professor
IEEE Senior Member
Department of Electrical Engineering,
École de Technologie Supérieure,
University of Quebec,
1100 Notre Dame West Street,
Montreal, Quebec H3C 1K3, Canada
e-mail: dessaint@ele.etsmtl.ca

Force Control Loop Affected by Bounded Uncertainties and Unbounded Inputs for Pneumatic Actuator Systems

The purpose of this paper is to develop an accurate closed-loop acting force technique for a pneumatic actuator, as an essential stage in the implementation of positioning control strategy. Since an analytical nonlinear structure, which linearly depends on parameter uncertainties, generically characterizes pneumatic plants, a feedback linearization design is proposed to cancel most of the resulting nonlinearities. Then, we proposed a linear state-feedback control and an additive nonlinear action to robustly bound the force error dynamics, devices which are required to handle the further parametric uncertainties and exogenous unbounded disturbances that will arise on the deduced structure. The design of the linear control gains is performed within robust closed-loop pole clustering using a linear matrix inequality approach. Finally, various experimental results illustrate the validity of the approach. [DOI: 10.1115/1.2807182]

Keywords: pneumatic actuator, acting force control, feedback, robustness, LMI

1 Introduction

The demand for pneumatic actuators for use in automation applications and mobile robots is growing [1]. Pneumatic systems provide a high degree of compliance, as well as dexterity, high speed, and force generation [2–4]. Therefore, cheap air supply is available everywhere in industrial surroundings [2,3]. However, their principal drawbacks, the significant compressibility of air and nonlinearities in the servovalves, hamper their considerable actuation capability [4–6]. Moreover, varying thermodynamic conditions (temperature, density, etc.) causes an appreciable change in a number of the model's parameters. An accurate model plant of a standard pneumatic system must induce certain features, such as higher nonlinearities and varying thermodynamic parameters [4,6,7]. In Ref. [8], the authors developed an effective pressure-controlled pneumatic system, employing a model that included 20–100 Hz frequency valve dynamics and nonlinear characteristics of the compressible flow through valve. Later, they proposed an effective procedure to develop a class of accurate models of pneumatic devices [4]. They addressed this issue by considering theoretical concepts (thermodynamics, fluid dynamics, etc.) under practical conditions (technological limitation, design, etc.).

More recently, these accurate models have been the subject of numerous papers on control strategies for pneumatic actuators. In particular, the most common problem in pneumatic actuator positioning is the complexity of the pneumatic and mechanical parts caused by the simultaneous occurrence of the flow of compressible fluid and the unavoidable friction behavior [5,6,9]. A natural way to investigate a performed control strategy is to separate the problem of pressure from that of position loops [10–13]. However, unfortunately, the coupling between the mechanical and pneumatic parts cannot be neglected by using singular perturbation theory, since the pneumatic part is too slow. Moreover, when the pressure control problem is considered independently of the position control problem, the perturbation caused by the motion of the mechanical part cannot be assumed to be bounded.

In many of these contributions (e.g., Refs. [7,8,14–17]), the pressure control loop is viewed as an important subproblem. In fact, many modern robot control algorithms (e.g., flapper-valve actuator in stewart platforms and other parallel actuation devices) require the ability to control directly the actuator output force or torque for compliant motions and when a specified end-point force is desired (as for many assembly operations and haptic interfaces) [1,14]. This force can be obtained by an inner acting force control loop (which is equivalent to the pressure drop control). More specifically, an efficient motion tracking can be ensured by combining an inner pressure feedback linearization control loop with an outer position one [11,18].

The pressure feedback linearization is often established to nullify the known nonlinearity arising from the compressibility of air and the mass flow dynamics by assuming the nominal statement on the pressure dynamics and by omitting the other nonlinear uncertainties [10,11] contained in the following different statements: (a) the temperature throughout the flow path of the valve is considered constant; (b) the discharge coefficient is considered to be constant and exactly known; (c) the effect of the load motion on the cylinder pressure dynamics is neglected, even if the load is moving; (d) the mass flow rate range is as large as possible, in order to maximize the piston speed and then to satisfy the omission of the friction dynamics [10,11,14,19]. So, by using any classical input-output feedback linearization technique, the control law is explicitly developed dependently on the nominal expression of the mass flow rate to get the linear model. However, the stabilization feedback remains in these cases rarely robust on the different kinds of disturbances and unknown variations. To overcome this robustness limitation, the authors proposed in Refs. [14,19] a

[1]Corresponding author.

Contributed by the Dynamic Systems, Measurement, and Control Division of ASME for publication in the JOURNAL OF DYNAMIC SYSTEMS, MEASUREMENT, AND CONTROL. Manuscript received February 13, 2006; final manuscript received June 4, 2007; published online December 18, 2007. Review conducted by Kim Stelson.

control law based upon an equilibrium pressure ratio and a local linearization procedure, which is robust with respect to the mass flow rate but only around a desired equilibrium point. In addition, the dynamical performances (rapidity and damping) are not taken into account in the control design in Ref. [19].

Then, to focus on the robustness consideration of the force control-loop, Richer and Hurmuzlu [9] choose the sliding mode control implementation, even though the model of the pneumatic plant that they investigate encounters some limitations and simplified assumptions: a constant valve discharge coefficient and a static friction compensation into the piston motion [15]. However, a specific drawback presented by the sliding mode techniques is that the magnitude of the control current and the fluctuations in the signal are large. Attempts to improve the tracking performance by increasing the controller gain is not fruitful because they lead to chattering, which is generally perceived as an oscillation around the sliding manifold [20]. This phenomenon is undesirable and seems to be responsible for the lifetime drop of some components (especially the servovalve) [20].

In Ref. [7], a robust pressure control scheme for a pneumatic servo system containing unknown possible nonlinear uncertainties was developed. Then, an implementation of a force control scheme was proposed [17], which is described as a feedback linearization technique applied on the analytical nonlinear structure. Such a structure depends linearly on parameter uncertainties, a generic characteristic of pneumatic plants. Moreover, parametric uncertainties and exogenous bounded disturbances arise on the deduced linear structure. Then, multiobjective constrained H_∞ and peak-to-peak gain minimizations were performed and compared.

A pressure control loop has also been proposed for a class of pneumatic systems for which the connection port comprises a non-negligible restriction [16,18]. In this case, the pressure in the cylinder cannot be directly measured and cannot be expressed as an explicit function of the measurable pressure [21]. The approach is based on the nonlinear observer design presented in Ref. [22] for estimating the internal pressure. Accordingly, a modified feedback linearization is combined with time-varying system stabilization to control the pressure in the cylinder chamber [21].

Nevertheless, no work holds on the case of unbounded uncertainties to deal with the design of the inner pressure loop. Even so, when we use this kind of loop as a control signal through any outer position loop, some significant signals as the motion rate cannot be assumed to be bounded a priori. Indeed, this statement requires a much more skilful design that coheres simultaneously with the force and position control loops. This remains particularly important in the case of pneumatic actuators because of the slowness of their pressure dynamics, which are consequently coupled with the motion behavior.

In this paper, an acting force controller is proposed for the treatment of both bounded parametric uncertainties, due to thermodynamics (temperature, heat transfer and density), fluidic process (valve discharge characteristics), and a priori unbounded exogenous inputs (load motion and friction behavior) in the context of the unperformed positioning control of a pneumatic actuator under friction. To this end, we propose almost the same state-feedback linearization as given in Ref. [17] to cancel most of the nonlinearities, and we extend the approach to take into account the case of unlimited disturbances. Then, the remaining system is investigated by a linear controller and a nonlinear action to attenuate the level of unbounded known inputs. As in Refs. [7,17], the synthesis of the linear controller gains is based on an appropriate closed-loop pole location, expressed in terms of linear matrix inequalities (LMIs). Finally, various experimental results illustrate the validity of the approach.

The present paper is organized as follows. Section 2 provides a list of the nomenclature and notations used in this paper. In Sec. 3, we describe the system we are considering and set forth our assumptions, which are widely accepted in practice to design pneumatic plants. Then, we introduce our model of the pneumatic actuator force dynamics controller and describe the acting force controller's components in Sec. 4. Section 5 details the LMI synthesis of the linear state-feedback controller gains. A real-time implementation is presented in Sec. 6 to elaborate the various results and to illustrate the validity of our approach. Finally, concluding remarks are provided in Sec. 7.

Table 1 Nomenclature

Symbol	Description
m	Combined mass of piston and load
p_{cr}	Critical pressure ratio
u	Valve spool position
x, $\dot{x}$	Cylinder piston position and velocity
C_d	Discharge coefficient of the valve
P_i, P_l, P_r	Inner, left-chamber, and right-chamber cylinder absolute pressures
P_o, P_e, P_s	Outer, exhaust, and supply absolute pressures
R	Ideal gas constant
S_l, S_r	Piston cross-sectional areas of the left and right ports
T_a	Ambient absolute temperature
V_l, V_r	Left-chamber and right-chamber volumes
W	Spool constant
α, β	Parameters uncertainties
ζ	Ratio of specific heats
τ	Parameter used for modeling the temperature variation

2 Nomenclature

The variables and parameters of the plant are defined in Table 1.

3 Pneumatic Actuator Modeling

3.1 System Description and Assumptions. The system we consider here consists of a cylinder controlled with a current-actuated servovalve (see Fig. 1). We assume the following [1,4,7,23]:

- the gas is ideal;
- the air chamber's thermodynamic states (pressure, temperature, and density) are uniform;
- the entire system's air temperature varies slightly from its nominal value;
- the turbulent flow process behaves somewhere between isothermally and adiabatically;
- the flow leakages are negligible;
- the motion of the {piston+rod+load} assembly may be conducted under friction;
- the volume of each chamber and its instantaneous variations are easily measured time-varying characteristics;
- the servovalve dynamics are negligible;

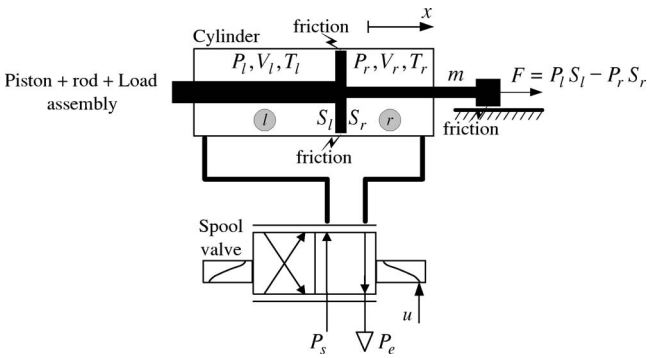

Fig. 1 Pneumatic system scheme

- the servovalve is characterized by one uncertain discharge coefficient.

3.2 Pressure Force Dynamics. Below, we derive a nonlinear state-space model, which is, in particular, linear in the control input u, with structured uncertainties for the rate change of the pressures in the chambers (see Fig. 1) based on the previous assumptions [1,7,23], for $i=l,r$ and $o=e,s$:

$$\dot{P}_i = -\alpha(t)g_i(P_i,x,\dot{x}) + \beta(t)h_i(t,P_i,x)u \tag{1}$$

where

$$g_i(P_i,x,\dot{x}) = \frac{P_i\dot{V}_i(\dot{x})}{V_i(x)} \tag{2}$$

and

$$h_i(t,P_i,x) = \frac{\sqrt{RT_a}}{V_i(x)}Wf(P_i)\mathrm{sgn}(u) \tag{3}$$

with

$$f(P_i) = \begin{cases} -P_i\bar{f}\left(\dfrac{P_o}{P_i}\right) | P_i > P_o \\ P_o\bar{f}\left(\dfrac{P_i}{P_o}\right) | P_i \le P_o \end{cases} \tag{4}$$

where $\bar{f}$ designates the reduced flow function and is given by Refs. [1,4]:

$$\bar{f}(p) = \begin{cases} C_1 & \text{if } p \le p_{\mathrm{cr}} \\ C_2 p^{1/\zeta}\sqrt{1-p^{\zeta-1/\zeta}} & \text{if } p > p_{\mathrm{cr}} \end{cases} \tag{5}$$

with constants

$$C_1 = \sqrt{\frac{\zeta}{R}\left(\frac{2}{\zeta+1}\right)^{\zeta+1/\zeta-1}} \quad C_2 = \sqrt{\frac{2\zeta}{R(\zeta-1)}} \quad \text{and}$$

$$p_{\mathrm{cr}} = \left(\frac{2}{\zeta+1}\right)^{\zeta/\zeta+1} \tag{6}$$

$\alpha(\cdot)$ denotes the uncertain heat coefficient, which takes values between 1 and ζ (see Table 1) and depends on the actual heat transfer occurring during the process [4]; $\beta(\cdot)$ is an uncertain bounded parameter used to characterize the combination of the heat coefficient $\alpha(\cdot)$, the unknown valve discharge coefficient $C_d(\cdot)$, and the variation of the temperature $\tau(\cdot)$ [4,23]; $\beta(\cdot)$ is generically expressed by

$$\beta(t) = \alpha(t)C_d(t)\sqrt{\tau(t)} \tag{7}$$

Then, the first-time derivative of the force produced by the actuator $F=P_lS_l-P_rS_r$ (see Fig. 1) can be expressed as follows [1]:

$$\dot{F} = -\alpha(t)g(P_l,P_r,x,\dot{x}) + \beta(t)h(t,P_l,P_r,x)u \tag{8}$$

The functions $g(\cdot,\cdot,\cdot,\cdot)$ and $h(\cdot,\cdot,\cdot,\cdot)$ are found to be

$$g(P_l,P_r,x,\dot{x}) = g_l(P_l,x,\dot{x})S_l - g_r(P_r,x,\dot{x})S_r \tag{9}$$

and

$$h(t,P_l,P_r,x) = h_l(t,P_l,x)S_l - h_r(t,P_r,x)S_r \tag{10}$$

In Eq. (10), we use Eq. (4) such that if $o=e$ when $i=l$ (i.e., the left chamber is opened to the atmosphere), then we have $o=s$ when $i=r$ (i.e., the right chamber is connected to the supply) and vice versa.

4 Acting Force Controller

In this section, we propose a controller design for the force actuated on the mechanical part of the pneumatic actuator under friction. However, the friction compensation is not included here as it is investigated inside a position control loop in a separate paper. Thus, we develop the acting force controller design using nonlinear plants to cancel most of the nonlinearities. A simple proportional integral (PI) controller combined with a nonlinear damping compensator is proposed, despite the remaining unbounded measured elements, to robustly stabilize the force error dynamics.

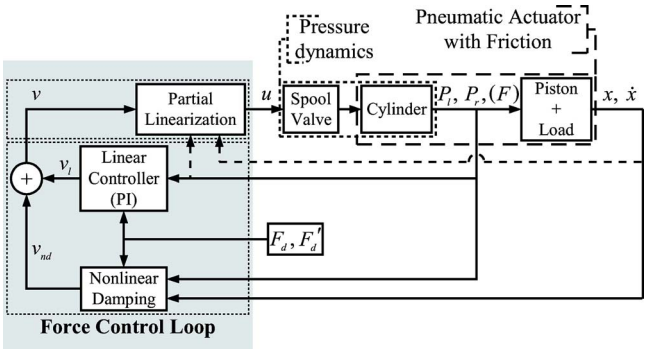

Fig. 2 Proposed control strategy

4.1 "Partial" Linearization. In order to efficiently apply a linear control law of the actuator output force F, we first propose the following feedback linearizing compensator (see Fig. 2) [17]:

$$u = \frac{v + \alpha_n g(P_l,P_r,x,\dot{x})}{\beta_n h(t,P_l,P_r,x)} \tag{11}$$

where α_n is an "additive" nominal value of α, that is, $\alpha=\alpha_n+\tilde{\alpha}$, and β_n is a "multiplicative" value of β, that is, $\beta=\beta_n\cdot\tilde{\beta}$. The choice of these nominal values and the shapes of their relative uncertainties (an additive variation associated with the one and a multiplicative variation to the other) are stated to make profit to the linearization feedback (11). Indeed, the effect of these relative uncertainties on the deduced error dynamics will be limited, thanks to their reduced magnitudes. We will discuss, once again, in connection with this statement, in the following section when we present the linear controller and the nonlinear damping action. So, we release system (8) of most known nonlinear dynamics by replacing Eq. (11) in Eq. (8):

$$\dot{F}(t) = \pi_1(t)g(P_l,P_r,x,\dot{x}) + \tilde{\beta}(t)v \tag{12}$$

where $\pi_1(t)=-\alpha(t)+\alpha_n\tilde{\beta}(t)$. The term g, given by Eq. (9), is a function of known states: the pressure, which is bounded, the position, and particularly the velocity, which are not bounded a priori. So, the use of any optimization criterion, as given in Ref. [17], is not appropriate here, and the force dynamics (12) cannot be treated only by using a linear compensator. We complete the design of the force controller below.

4.2 PI+Nonlinear Damping Compensator. The control objective is for the actuator output force F to track a specific time-varying force. For instance, when dealing with the positioning problem under friction, this force reference becomes, in addition, a function of the velocity variable and a combination of friction force estimates [24]. In the following, let $F_d(t,\dot{x})$ be the force reference, $\tilde{F}=F-F_d$ the tracking error, and $\mathbf{X}=(\int\tilde{F}dt\ \tilde{F})^T$ the vector of force error states. The tracking system model for the pneumatic force is then given in the following stated representation:

$$\dot{\mathbf{X}} = \mathbf{A}\mathbf{X} + \mathbf{B}\cdot(\tilde{\beta}v + \pi_1 g - \dot{F}_d) \tag{13}$$

with

$$\mathbf{A}=\begin{pmatrix}0 & 1\\ 0 & 0\end{pmatrix} \quad \text{and} \quad \mathbf{B}=\begin{pmatrix}0\\ 1\end{pmatrix}$$

In particular, in accordance with the modeling of the friction force and its estimate commonly found in the literature, and by convenience, we can write the tracking reference differentiation as a combination of continuous and discontinuous terms, as follows (see Ref. [24] for details):

$$\dot{F}_d(t,\dot{x}) = F'_d(t,\dot{x}) - \pi_2(\dot{x})\Theta(t,\dot{x}) \tag{14}$$

where $F'_d(t,\dot{x})$ denotes a continuous approximation of the tracking reference derivative, and $\pi_2(\dot{x})\Theta(t,\dot{x})$ its approximation error. $\Theta(t,\dot{x})$ is a continuous function and $\pi_2(\dot{x})$ is an uncertain parameter, and includes the discontinuity feature around zero velocity (see in Ref. [24]). For instance, if we suggest a friction compensation based on the *LuGre* model, we meet this kind of discontinuity in its derivative (see Appendix). We note that this friction model is used to encounter the most of static and dynamic characteristics of friction bahavior [25,26]. The friction compensation is particularly combined with any position control loop, which is not treated in this paper. However, the differentiation term $\dot{F}_d(t,\dot{x})$ introduced in Eq. (14) remains close to the objective of that position loop.

The following controller design is based on the well-known nonlinear damping approach [27], which is robustly applied within a multiplicative uncertainty component (the term $\tilde{\beta}$ in Eq. (13)).

PROPOSITION. *Consider system (12). If the control action v is finely defined as a combination of two terms (see Figure 2):*

$$v = v_l + v_{nd} \tag{15}$$

where

$$v_l = F'_d - \mathbf{K}\mathbf{X} \tag{16}$$

and

$$v_{nd} = -\kappa(g^2 + F'^2_d + \Theta^2)\mathbf{B}^T\mathbf{P}^{-1}\mathbf{X} \tag{17}$$

Then the closed-loop system is uniformly bounded. v_l is the term that is linearly dependent on the errors and the continuous feedforward term F'_d, and v_{nd} is the nonlinear damping term, but smoothed to compensate for exogenous inputs of the closed-loop force dynamics. Moreover, the state-feedback $\mathbf{K}\mathbf{X}$ is introduced such that there exists a unique positive definite and symmetrical matrix $\mathbf{P}$ for a given positive definite and symmetrical $\mathbf{Q}_{\tilde{\beta}}$ to the Lyapunov equations:

$$(\mathbf{A} - \tilde{\beta}\mathbf{B}\mathbf{K})\mathbf{P} + \mathbf{P}(\mathbf{A} - \tilde{\beta}\mathbf{B}\mathbf{K})^T + \mathbf{Q}_{\tilde{\beta}} = 0 \tag{18}$$

for any $\tilde{\beta} \in [\underline{\tilde{\beta}}, \bar{\tilde{\beta}}]$. Finally, we choose $\kappa > 0$ in (17).

Proof. The substitution of Eqs. (14) and (15), and then Eq. (16), into Eq. (13) yields the following state error dynamics:

$$\dot{\mathbf{X}} = (\mathbf{A} - \tilde{\beta}\mathbf{B}\mathbf{K})\mathbf{X} + \mathbf{B}(\tilde{\beta}v_{nd} + \pi_1 g + \pi_2\Theta + \pi_3 F'_d)$$

with $\pi_3 = \tilde{\beta} - 1$.

Choose the Lyapunov function candidate for this system as $V = \frac{1}{2}\mathbf{X}^T\mathbf{P}^{-1}\mathbf{X}$. Then, the time derivative of V along the solution of the system will be

$$\dot{V} = \frac{1}{2}\mathbf{X}^T[\mathbf{P}^{-1}(\mathbf{A} - \tilde{\beta}\mathbf{B}\mathbf{K}) + (\mathbf{A} - \tilde{\beta}\mathbf{B}\mathbf{K})^T\mathbf{P}^{-1}]\mathbf{X} + \mathbf{X}^T\mathbf{P}^{-1}[\mathbf{B}(\tilde{\beta}v_{nd} + \pi_1 g + \pi_2\Theta + \pi_3 F'_d)] \leqslant -\frac{1}{2}\mathbf{X}^T\mathbf{P}^{-1}\mathbf{Q}_{\tilde{\beta}}\mathbf{P}^{-1}\mathbf{X} + \mathbf{X}^T\mathbf{P}^{-1}\mathbf{B}\tilde{\beta}v_{nd} + \bar{\pi}_1|\mathbf{X}^T\mathbf{P}^{-1}\mathbf{B}g| + \bar{\pi}_2|\mathbf{X}^T\mathbf{P}^{-1}\mathbf{B}\Theta| + \bar{\pi}_3|\mathbf{X}^T\mathbf{P}^{-1}\mathbf{B}F'_d|$$

with $\bar{\pi}_1 = \max(|\pi_1|) \geqslant |\pi_1|$, $\bar{\pi}_2 = \max(|\pi_2|) \geqslant |\pi_2|$ and $\bar{\pi}_3 = \max(|\pi_3|) \geqslant |\pi_3|$. Next, define

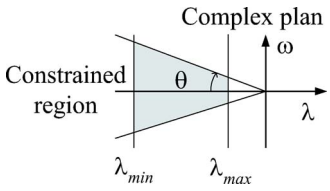

Fig. 3 Stability region $\mathcal{D}$

$$v_{nd} = -\frac{1}{\underline{\tilde{\beta}}}(\kappa_1 g^2 + \kappa_2\Theta^2 + \kappa_3 F'^2_d)\mathbf{B}^T\mathbf{P}^{-1}\mathbf{X}$$

Then, we have

$$\dot{V} \leqslant -\frac{1}{2}\mathbf{X}^T\mathbf{P}^{-1}\mathbf{Q}_{\tilde{\beta}}\mathbf{P}^{-1}\mathbf{X} - \kappa_1|\mathbf{B}^T\mathbf{P}^{-1}\mathbf{X}|^2|g|^2 + \bar{\pi}_1|\mathbf{B}^T\mathbf{P}^{-1}\mathbf{X}||g| - \kappa_2|\mathbf{B}^T\mathbf{P}^{-1}\mathbf{X}|^2|\Theta|^2 + \bar{\pi}_2|\mathbf{B}^T\mathbf{P}^{-1}\mathbf{X}||\Theta| - \kappa_3|\mathbf{B}^T\mathbf{P}^{-1}\mathbf{X}|^2|F'_d|^2 + \bar{\pi}_3|\mathbf{B}^T\mathbf{P}^{-1}\mathbf{X}||F'_d|$$

The term $-\kappa_1|\mathbf{B}^T\mathbf{P}^{-1}\mathbf{X}|^2|g|^2 + \bar{\pi}_1|\mathbf{B}^T\mathbf{P}^{-1}\mathbf{X}\|g|$ has a maximum of $\bar{\pi}_1^2/4\kappa_1$ at $|\mathbf{B}^T\mathbf{P}^{-1}\mathbf{X}\|g| = \bar{\pi}_1/2\kappa_1$. The term $-\kappa_2|\mathbf{B}^T\mathbf{P}^{-1}\mathbf{X}|^2|\Theta|^2 + \bar{\pi}_2|\mathbf{B}^T\mathbf{P}^{-1}\mathbf{X}\|\Theta|$ has a maximum of $\bar{\pi}_2^2/4\kappa_2$ at $|\mathbf{B}^T\mathbf{P}^{-1}\mathbf{X}\|\Theta| = \bar{\pi}_2/2\kappa_2$. Finally, the term $-\kappa_3|\mathbf{B}^T\mathbf{P}^{-1}\mathbf{X}|^2|F'_d|^2 + \bar{\pi}_3|\mathbf{B}^T\mathbf{P}^{-1}\mathbf{X}\|F'_d|$ has a maximum of $\bar{\pi}_3^2/4\kappa_3$ at $|\mathbf{B}^T\mathbf{P}^{-1}\mathbf{X}\|F'_d| = \bar{\pi}_3/2\kappa_3$. Then

$$\dot{V} \leqslant -\frac{1}{2}\mathbf{X}^T\mathbf{P}^{-1}\mathbf{Q}_{\tilde{\beta}}\mathbf{P}^{-1}\mathbf{X} + \frac{\bar{\pi}_1^2}{4\kappa_1} + \frac{\bar{\pi}_2^2}{4\kappa_2} + \frac{\bar{\pi}_3^2}{4\kappa_3}$$

$\dot{V}$ is negative outside some ball (see Lemma 14.1 in Ref. [27]). It follows from Theorem 4.18 in Ref. [27] that, for any initial state $\mathbf{X}(t_0)$, the solution of the closed-loop system is uniformly bounded. Finally, we choose $\kappa = 1/\underline{\tilde{\beta}}\max(\kappa_1, \kappa_2, \kappa_3)$. ■

We note that, in the previous controller modelization introduced in Sec. 3.2, the two additive and multiplicative uncertain variations are contained in the nonlinear damping design as they appear in the a priori unbounded terms (see π_1 and π_3 in the proof given above and in Eq. (13)). On the other hand, according to the force error dynamics (13) and thanks to the feedback linearizing compensator (11), the linear part of these dynamics depends only on the uncertainty variation $\tilde{\beta}$. On the contrary, if all the nonlinear dynamic terms are considered to be bounded, we attempt to obtain a completely linear dynamics combining the two kinds of uncertainties stated above (i.e., α and β). This problem statement is widely discussed in previous works (see in Refs. [7,17]).

5 Linear State-Feedback Synthesis

The set of Lyapunov equations (18) means that the linear part of the closed-loop system, given by Eqs. (13) and (15)–(17), is uniformly asymptotically stable. Moreover, this item can be numerically solved by using LMI frameworks. In addition, for a robust synthesis, which takes into account the structured bounded uncertainties [28], the linear part of the closed-loop system, i.e., $\dot{\mathbf{X}} = (\mathbf{A} - \tilde{\beta}\mathbf{B}\mathbf{K})\mathbf{X}$, can have a specific decay rate and maximum possible damping in all modes, and prevent fast controller dynamics. That being so, a multiobjective controller design will be formulated as a pole clustering feasibility problem in a $\mathcal{D}$-stability region involving LMIs. Thereafter, the closed-loop stability condition (18) will be replaced by the $\mathcal{D}$-stability (see Fig. 3) given by [28,29]

$$\mathcal{D}(\lambda_{\min}, \lambda_{\max}, \theta) \triangleq \{\lambda + j\omega \in \mathbb{C} | \lambda_{\min} \leqslant \lambda \leqslant \lambda_{\max} \tan\theta \cdot \lambda < -|\omega|\} \tag{19}$$

for chosen $\lambda_{\min}$, $\lambda_{\max}$, and θ. Meanwhile, confining the closed-loop poles to this subregion bounds the settling time, the frequency of oscillatory modes (by considering vertical strips), and

the maximum overshoot (by considering conic sectors), respectively. Firstly, denote by $\mathcal{L}^+$ and $\mathcal{L}^-$ the following matricial operators:

$$\mathcal{L}^+(\mathbf{X}_1,\mathbf{Y}_1,\mathbf{X}_2,\mathbf{Y}_2) = (\mathbf{X}_1\mathbf{Y}_1 + \mathbf{Y}_1^T\mathbf{X}_1^T) - (\mathbf{X}_2\mathbf{Y}_2 + \mathbf{Y}_2^T\mathbf{X}_2^T)$$

and

$$\mathcal{L}^-(\mathbf{X}_1,\mathbf{Y}_1,\mathbf{X}_2,\mathbf{Y}_2) = (\mathbf{X}_1\mathbf{Y}_1 - \mathbf{Y}_1^T\mathbf{X}_1^T) - (\mathbf{X}_2\mathbf{Y}_2 - \mathbf{Y}_2^T\mathbf{X}_2^T)$$

By using the LMI regions [29], the $\mathcal{D}$ stability of the linear part of the error force dynamics can be reduced to the following matrix inequality statements: $\forall \tilde{\beta} \in [\underline{\tilde{\beta}}, \bar{\tilde{\beta}}]$,

$$\mathbf{P} > 0 \tag{20}$$

$$\mathcal{L}^+(\mathbf{A},\mathbf{P},\tilde{\beta}\mathbf{B}\mathbf{K},\mathbf{P}) - 2\lambda_{\min}\mathbf{P} > 0 \tag{21}$$

$$\mathcal{L}^+(\mathbf{A},\mathbf{P},\tilde{\beta}\mathbf{B}\mathbf{K},\mathbf{P}) - 2\lambda_{\max}\mathbf{P} < 0 \tag{22}$$

and

$$\begin{bmatrix} \sin\theta\,\mathcal{L}^+(\mathbf{A},\mathbf{P},\tilde{\beta}\mathbf{B}\mathbf{K},\mathbf{P}) & \cos\theta\,\mathcal{L}^-(\mathbf{A},\mathbf{P},\tilde{\beta}\mathbf{B}\mathbf{K},\mathbf{P}) \\ -\cos\theta\,\mathcal{L}^-(\mathbf{A},\mathbf{P},\tilde{\beta}\mathbf{B}\mathbf{K},\mathbf{P}) & \sin\theta\,\mathcal{L}^+(\mathbf{A},\mathbf{P},\tilde{\beta}\mathbf{B}\mathbf{K},\mathbf{P}) \end{bmatrix} < 0 \tag{23}$$

the variables of which are the symmetrical Lyapunov matrix $\mathbf{P}$ and the gain matrix $\mathbf{K}$, respectively. Since expressions in Eqs. (20)–(23) involve nonlinear terms of the form $\mathbf{BKP}$, the resulting feasibility problem is nonlinear. However, the LMI formulation is readily restored by rewriting Eqs. (20)–(23) in terms of $\mathbf{P}$ and the auxiliary variable $\mathbf{W}=\mathbf{KP}$ [30]. The given LMIs are, in fact, linear in variables $\mathbf{P}$ and $\mathbf{W}$. Now, observe that the closed-loop system is a linear parameter-dependent system (PDS) with respect to $\tilde{\beta}$, which is included in the convex set $[\underline{\tilde{\beta}}, \bar{\tilde{\beta}}]$. That being so, the LMIs are given equivalently by the following: for $k=1,2$;

$$\mathbf{P} > 0 \tag{24}$$

$$\mathcal{L}_k^+ - 2\lambda_{\min}\mathbf{P} > 0 \tag{25}$$

$$\mathcal{L}_k^+ - 2\lambda_{\max}\mathbf{P} < 0 \tag{26}$$

$$\begin{bmatrix} \sin\theta\,\mathcal{L}_k^+ & \cos\theta\,\mathcal{L}_k^- \\ -\cos\theta\,\mathcal{L}_k^- & \sin\theta\,\mathcal{L}_k^+ \end{bmatrix} < 0 \tag{27}$$

where

$$\mathcal{L}_1^+ = \mathcal{L}^+(\mathbf{A},\mathbf{P},\underline{\tilde{\beta}}\mathbf{B},\mathbf{W}) \quad \mathcal{L}_1^- = \mathcal{L}^-(\mathbf{A},\mathbf{P},\underline{\tilde{\beta}}\mathbf{B},\mathbf{W})$$

$$\mathcal{L}_2^+ = \mathcal{L}^+(\mathbf{A},\mathbf{P},\bar{\tilde{\beta}}\mathbf{B},\mathbf{W}) \quad \mathcal{L}_2^- = \mathcal{L}^-(\mathbf{A},\mathbf{P},\bar{\tilde{\beta}}\mathbf{B},\mathbf{W})$$

6 Experimental Results

The effectiveness of the proposed acting force control is illustrated by results of the implementation of an experimental system (see Fig. 4) consisting of a rodless cylinder (FESTO, DGP-25-500) controlled with a current actuated servovalve (FESTO, MPYE-5-1/8LF-010B). The valve critical frequency (which corresponds to the 3 dB frequency at the maximum movement stroke of the piston spool) is of 100 Hz (see in proportional valves MPYE technical data sheet). So, the valve dynamics that controls the flow to either side of the actuator can simply be neglected as previously stated in Sec. 3.1 [8,31]. The air supply is tuned via a regulator model (FESTO, LFR-M2-G1/4-C10RG). Pressure sensors (FESTO, SDE-10) are used to measure the pressure drop throughout the nonrestrictive ports (which is equivalent to the actual acting force, i.e., $F=S(P_l-P_r)$). The piston displacement is measured with a position sensor (FESTO, MLD-POT-500-TLF).

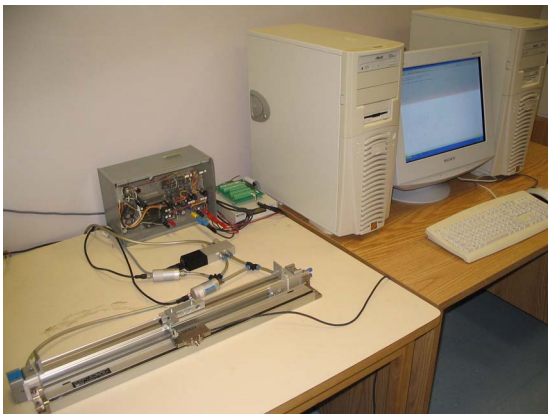

Fig. 4 Photo of the experimental setup

The velocity is obtained by differentiating and digitally filtering the position measurements. The experimental setup produces a quite higher and variational (stick and slip) friction behavior (static frcition $f_s \simeq 60$ N, Coulomb friction $f_c \simeq 40$ N and viscous coefficient $\sigma_2 \simeq 150$ N s/m). We have developed an estimation procedure of the friction parameters in the same setup in a previous work [26]. The spool valve displacement and the sensor measurements are, respectively, sent and received through an acquisition card (PCI-6052E). The control algorithm is implemented using XPC-SIMULINK software and the MATLAB© Real-Time-Workshop, with a sampling period of 100 μs.

The system parameters are given in Table 2. To ensure the $\mathcal{D}$ stability (see Fig. 3) of the uncertain linear part of the system, we choose the following stability region bounds: $\lambda_{\min}=-120$, $\lambda_{\max}=-2$, and $\theta=\arccos 0.7$. This is a compromise between the settling time of the response, the frequency of the oscillatory modes, the nonsaturation of the control effort, and the maximum overshoot. The LMIs (24)–(27) have been implemented using the MATLAB© LMI Toolbox [32]. We obtain the following linear controller gains: $\mathbf{K}=[177.8;74.9]$.

Numerous experiments are developed to illustrate the effectiveness of the proposed control design and to compare it with a pure linear robust compensation especially investigated in Ref. [33]. The main idea of this second alternative is to convert all the nonlinearities and uncertainties onto convex and bounded constraints upon the linear pressure dynamics by neglecting volume variation (i.e., load motion) in each cylinder chamber. On the deduced uncertain and linear dynamics, the completely PI linear controller is synthesized by using LMI formulation. We use the same pole clustering constraints applied on the linear part of our proposed approach to ensure the similar context for the two strategies compared here. Thus, we obtain in this case the following PI control

Table 2 Numerical values

Parameter	Lower value	Upper value	Nominal value
m (kg)	—	—	0.326
$u_{\max}$ (m)	—	—	0.002
P_e (kPa)	—	—	101
P_s (kPa)	—	—	608
R (N m/kg K)	—	—	287
$S_l=S_r$ (m^2)	—	—	4.9×10^{-4}
T_a (K)	—	—	295
$V_{c_{\max}}$ (m^3)	—	—	2.45×10^{-4}
W (m)	—	—	0.005
α	1.0	1.3997	1.1999
β	0.075	1.3297	0.7023
ζ	—	—	1.3997

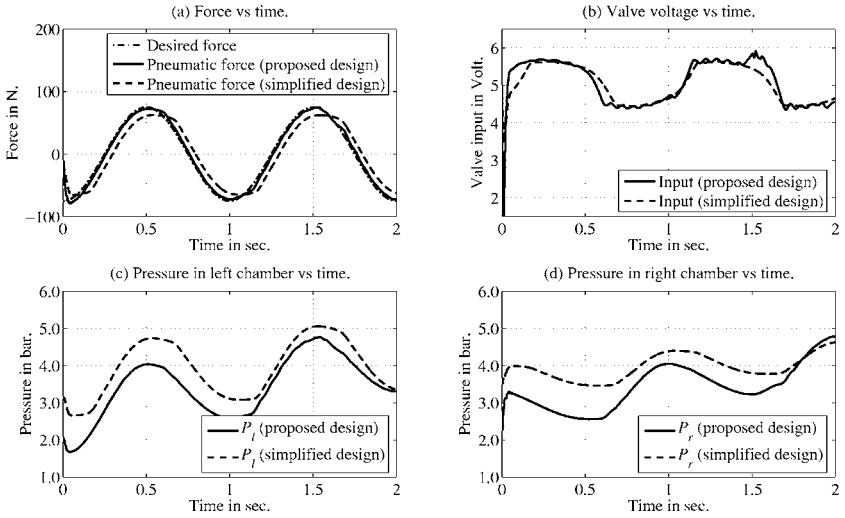

Fig. 5 Force control performance for a sine-force reference of 75 N−1 Hz

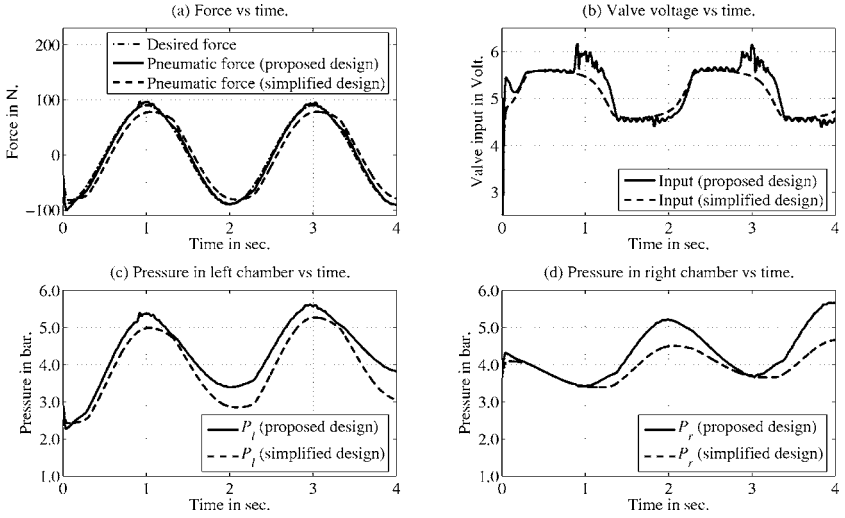

Fig. 6 Force control performance for a sine-force reference 90 N−0.5 Hz

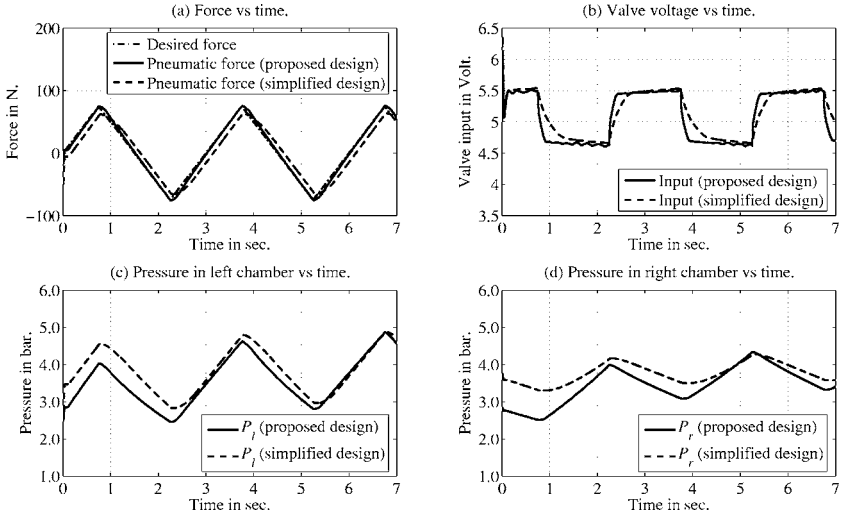

Fig. 7 Force control performance for a triangle-force reference

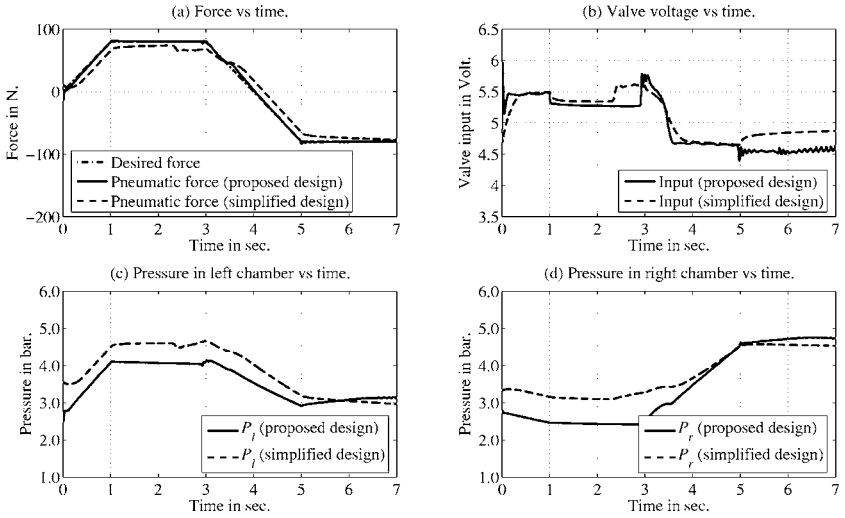

Fig. 8 Force control performance for a tooth-force reference

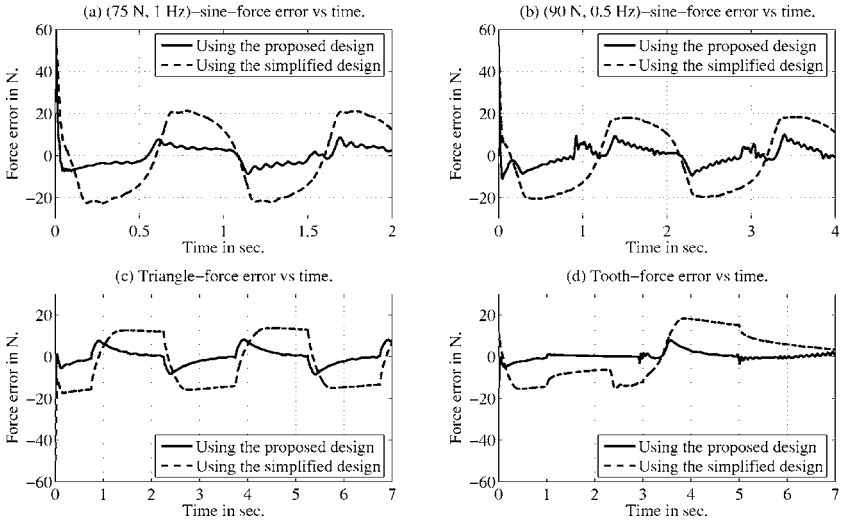

Fig. 9 Force error for different force references

gains: $K_p = 11.17 \times 10^{-6}$ and $K_i = 3.21 \times 10^{-6}$. In this case, the gains are very small because of the nonlinear dynamics, which are not compensated with any feedback linearization.

Next, we present the results obtained from a set of experiments conducted with different shapes of desired forces and, particularly, by varying the amplitudes and also the frequencies of sine waves, in order to observe the effect of their shapes and their rate variations. Figures 5(*a*), 6(*a*), 7(*a*), and 8(*a*) show the actual and desired forces of three different force reference trajectories. The error remains ultimately bounded. The corresponding control efforts displayed in Figs. 5(*b*), 6(*b*), 7(*b*), and 8(*b*) show that the spool valve voltage does not exceed the maximum value of 10 V (which is equivalent to the maximum spool displacement $u_{\max}$). In all cases, the control effort remains sufficiently smooth. The shapes of the input signal obtained with different desired force trajectories show the nonlinear behavior because the system is very nonlinear, especially when we are using our proposed control scheme, which contains appropriate nonlinear compensation terms. Figures 5(*c*), 6(*c*), 7(*c*), 8(*c*), 5(*d*), 6(*d*), 7(*d*), and 8(*d*) show the pressure levels in each chamber of the cylinder. As we can see, there is no fluctuation in these responses despite the small oscillations that appear in the corresponding control effort signals (due probably to the frequency response of the servovalve). However, there is no noise that can be heard during the experiment. The light drift observed on the evolution of the pressure in time does not critically affect the tracking performance or the stability feature, even if we lengthen the period of experiment. It is essentially caused by the piston motion and the asymmetry of the friction behavior during the motion in the two directions. Indeed, when the piston moves, the dynamics of the pressure in the chambers are more

Table 3 Peak and rms force errors using the two different force compensations (Design 1 for the proposed control design and Design 2 for the pure linear control) for sine inputs with various amplitudes (frequency of 1.0 Hz)

Amplitude (N)	Peak error (N)		rms error (N)	
	Design 1	Design 2	Design 1	Design 2
75	9.04	22.28	4.21	16.83
80	10.74	22.77	5.25	17.24
85	9.63	23.26	3.94	17.66
90	10.35	23.85	4.21	18.25
95	9.53	26.11	3.82	19.15
100	9.91	26.71	3.93	20.29

Table 4 Peak and rms force errors using the two different force compensations (Design 1 for the proposed control design and Design 2 for the pure linear control) for sine inputs with various frequencies (amplitude of 90.0 N)

Frequency (Hz)	Peak error (N)		rms error (N)	
	Design 1	Design 2	Design 1	Design 2
0.5	9.54	19.70	4.33	14.50
1.0	10.35	23.85	4.21	18.25
1.5	9.35	28.50	3.46	20.23
2.0	9.74	32.99	3.35	23.07
2.5	10.42	37.63	4.23	25.32
3.0	10.50	42.47	4.84	28.30

complex due to the changes in volume and the friction between the piston seals and the cylinder bore. Figure 9 recapitulates the error performance obtained by using the two comparative controllers within the different shaping forces. More complete results mapping the peak and rms errors for 1.0 Hz frequency-sine inputs with various amplitudes and 90.0 N magnitude-sine desired forces with various frequencies are illustrated in Tables 3 and 4, respectively. We can easily check the higher performances of our proposed strategy. The results obtained with the only PI control are more and more deteriorated as the the desired force variation rate is increasing. So, the proposed design becomes more efficient in this case. This means that the nonlinearities and parameter variations may dominate the system characteristics and make the tracking force variation difficult. The better the nonlinearity compensation, the smaller the tracking force error can be achieved for the uncertain and disturbed pneumatic actuator dynamics. It is obviously seen now that the only use of a linear controller is not sufficient for this kind of plants even though the gains are finely calculated to ensure the robustness with respect to all the possible uncertainties (including the specific higher nonlinearities of these systems).

7 Conclusion

In this paper, we have proposed a complete design of a pneumatic acting force control, taking into account bounded parametrical uncertainties and possible unbounded variables. This control loop is not necessary usable alone but it remains suitable for very demanding applications addressing the problem of piston motion control under friction. In fact, precise motion trajectory tracking can be obtained by combining a force feedback linearization inner loop with a position control loop. It is composed of a state-feedback, linearization to cancel most of the known nonlinearities, a robust linear state-feedback, and another nonlinear compensator to ultimately render the force error bounded. To this end, a detailed proof is established, and experimental results are presented. The force performance shown is sufficient to robustly compensate for motion driving under friction.

Appendix

In the context of a position tracking problem, the time-varying force objective F_d can be designed as a linear combination of three components: a feedforward term, a position feedback correction, and a friction force estimation. The first and the second terms are assumed to be sufficiently smooth and differentiable, whereas this is not the case for the third one through almost all the friction models. For instance, the powerful and complete LuGre friction model encounters a discontinuity in its derivative. A LuGre friction compensation can be stated as follows [24,25]:

$$\dot{\hat{z}} = -\frac{\sigma_0|\dot{x}|}{\varphi(\dot{x})}\hat{z} + \dot{x} + v_z$$

and

$$\hat{f}_{\text{fr}} = \sigma_0\hat{z} + \sigma_1\dot{\hat{z}} + \sigma_2\dot{x}$$

where

$$\varphi(\dot{x}) = f_c + (f_s - f_c)e^{-\dot{x}^2/\dot{x}_s^2}$$

where $\hat{z}$ is the internal friction estimate, $\hat{f}_{\text{fr}}$ is the friction force estimation, σ_0, σ_1 and σ_2 are the stiffness, the frictional damping and the viscous friction coefficients respectively. The term $\varphi(\dot{x})$ is a finite function chosen to describe the Stribeck effect [25]. The terms f_c and f_s correspond to the Coulomb friction and the stiction friction forces, respectively. The parameter $\dot{x}_s$ is the Stribeck relative velocity. v_z represents any observer dynamic feedback related to the measurable states of the position system (see in Refs. [25,34]).

The derivative of the friction force estimation is not rather continuous, as it contains the term $\sigma_0\sigma_1/\varphi(\dot{x})\hat{z}\ddot{x}\,\text{sgn}(\dot{x})$ [24]. This latter can be decomposed of a continuous approximation and its associated error, as follows:

$$\frac{\sigma_0\sigma_1}{\varphi(\dot{x})}\hat{z}\ddot{x}\,\text{sgn}(\dot{x}) = \frac{\sigma_0\sigma_1}{\varphi(\dot{x})}\hat{z}\ddot{x}\,\text{sat}(\dot{x}) - \pi_2(\dot{x})\Theta(t,\dot{x})$$

with

$$\Theta(t,\dot{x}) = \frac{\sigma_0\sigma_1}{\varphi(\dot{x})}\hat{z}\ddot{x}$$

and

$$\pi_2(\dot{x}) = \text{sat}(\dot{x}) - \text{sgn}(\dot{x})$$

Otherwise, we replace the sign function by the continuous function sat in the feedforward term $\dot{F}_d(t,\dot{x})$.

References

[1] Kazerooni, H., 2005, "Design and Analysis of Pneumatic Force Generators for Mobile Robotic Systems," IEEE/ASME Trans. Mechatron., **10**(4), pp. 411–418.

[2] André, P., Kauffmann, J.-M., Lhote, F., and Taillard, J.-P., 1983, *Les Robots—Constituants Technologiques—Tome 4*, Hermes, Paris.

[3] Vertut, J., and Coiffet, P., 1984, *Les Robots—Téléopération, Évolution des Technologies—Tome 3*, Hermes, Paris.

[4] Khayati, K., Bigras, P., and Dessaint, L.-A., 2003, "On Modelization and Robust Controller Synthesis of Pneumatic Actuator Plants Using LMI Approach," *IMACS Multiconference Computational Engineering in Systems Applications*, Lille, France, Paper No. S1-R-00–0304.

[5] Shearer, J. L., 1956, "Study of Pneumatic Processes in the Continuous Control of Motion With Compressed Air—I, II," Trans. ASME, **78**, pp. 233–249.

[6] Anderson, B. W., 1967, *The Analysis and Design of Pneumatic Systems*, Wiley, New York.

[7] Khayati, K., Bigras, P., and Dessaint, L.-A., 2002, "A Robust Pole Clustering Design of Pneumatic Systems Using LMI Approach," *Proceedings of the IEEE International Conference on Systems, Man and Cybernetics*, Hammamet, Tunisia, Vol. 4, pp. 274–279.

[8] Khayati, K., Bigras, P., and Dessaint, L.-A., 2002, "Retaining Or Neglecting Valve Spool Dynamics in Tracking Controller Strategies for Pneumatic Systems," *Proceedings of the IEEE International Conference on Methods and Models in Automation and Robotics*, Szczecin, Poland.

[9] Richer, E., and Hurmuzlu, Y., 2000, "High Performance Pneumatic Force Ac-

tuator System, Part I—Nonlinear Mathematical Model," ASME J. Dyn. Syst., Meas., Control, **122**(3), pp. 416–425.
[10] Song, J., and Ishida, Y., 1997, "A Robust Sliding Mode Control for Pneumatic Servo Systems," Int. J. Eng. Sci., **35**(8), pp. 711–723.
[11] Lee, H. K., Choi, G. S., and Choi, G. H., 2002, "A Study on Tracking Position Control of Pneumatic Actuators," Mechatronics, **12**(6), pp. 813–831.
[12] Xiang, F., and Wikander, J., 2004, "Block-Oriented Approximate Feedback Linearization for Control of Pneumatic Actuator System," IFAC J. Control Eng. Pract., **12**(4), pp. 387–399.
[13] Schulte, H., and Hahn, H., 2004, "Fuzzy State Feedback Gain Scheduling Control of Servo-Pneumatic Actuators," IFAC J. Control Eng. Pract., **12**(5), pp. 639–650.
[14] Ben-Dov, D., and Salcudean, S. E., 1995, "A Force Controlled Pneumatic Actuator," IEEE Trans. Rob. Autom., **11**(6), pp. 906–911.
[15] Richer, E., and Hurmuzlu, Y., 2000, "High Performance Pneumatic Force Actuator System: Part II—Nonlinear Controller Design," ASME J. Dyn. Syst., Meas., Control, **122**(3), pp. 426–434.
[16] Bigras, P., and Khayati, K., 2002, "Modified Feedback Linearization Controller for Pneumatic System With Non Negligible Connection Port Restriction," *Proceedings of the IEEE International Conference on Systems, Man and Cybernetics*, Hammamet, Tunisia, Vol. 2, pp. 227–231.
[17] Khayati, K., Bigras, P., and Dessaint, L.-A., 2004, "A Robust Feedback Linearization Force Control of a Pneumatic Actuator," *Proceedings of the IEEE International Conference on Systems, Man and Cybernetics*, The Hague, Holland, pp. 6113–6119.
[18] Bigras, P., 2005, "Controller Design for Pneumatic Systems With Connection Port Restriction: An LMI Approach," Trans. Can. Soc. Mech. Eng., **29**, pp. 23–40.
[19] Outbib, R., and Richard, E., 2000, "State Feedback Stabilization of an Electropneumatic System," ASME J. Dyn. Syst., Meas., Control, **122**(3), pp. 410–415.
[20] Smaoui, M., Brun, X., and Thomasset, D., 2006, "A Study on Tracking Position Control of an Electropneumatic System Using Backstepping Design," IFAC J. Control Eng. Pract., **14**, pp. 923–933.
[21] Bigras, P., 2005, "Pressure Control of Pneumatic Systems With a Non Negligible Connection Port Restriction," Control Intell. Syst., **33**, pp. 111–118.
[22] Bigras, P., and Khayati, K., 2002, "Nonlinear Observer for Pneumatic System With Non Negligible Connection Port Restriction," *Proceedings of the IEEE American Control Conference*, Anchorage, AK, pp. 3191–3195.
[23] Bigras, P., 2005, "Sliding-Mode Observer as a Time-Variant Estimator for Control of Pneumatic Systems," ASME J. Dyn. Syst., Meas., Control, **127**, pp. 499–502.
[24] Khayati, K., Bigras, P., and Dessaint, L.-A., 2006, "On Force Control of Pneumatic Actuator Subject to a Position Tracking and a Friction Estimation Based on *LuGre* Model," École de Technologie Supérieure, Technical Report No. ETS-RT-2006-001.
[25] Canudas, C. W., Olsson, H., Aström, K. J., and Lischinsky, P., 1995, "A New Model for Control of Systems With Friction," IEEE Trans. Autom. Control, **40**(3), pp. 419–425.
[26] Madi, M. S., Khayati, K., and Bigras, P., 2004, "Parameter Estimation for the *LuGre* Friction Model Using Interval Aanalysis and Set Inversion," *Proceedings of the IEEE International Conference on Systems, Man and Cybernetics*, The Hague, Holland, pp. 428–433.
[27] Khalil, H. K., 2002, *Nonlinear Systems*, Prentice-Hall, New York.
[28] Chilali, M., Gahinet, P., and Apkarian, P., 1999, "Robust Pole Placement in LMI Regions," IEEE Trans. Autom. Control, **44**(12), pp. 2257–2270.
[29] Chilali, M., and Gahinet, P., 1996, "H_∞ Design With Pole Placement Constraints: An LMI Approach," IEEE Trans. Autom. Control, **41**(3), pp. 358–367.
[30] Boyd, S., El Ghaoui, L., Feron, E., and Balakrishnan, V., 1994, *Linear Matrix Inequalities in Systems and Control Theory*, Society for Industrial and Applied Mathematics, Philadelphia, PA, Vol. 15.
[31] Khayati, K., Bigras, P., and Dessaint, L.-A., 2001, "Nonlinear Control of Pneumatic Actuators," *Proceedings of the ICC&IE International Conference on Computers and Industrial Engineering*, Montreal, pp. 214–218.
[32] Gahinet, P., Nemirovskii, A., Laub, A. J., and Chilali, M., 1995, *MATLAB LMI Control Toolbox*, The MathWorks Inc., MA.
[33] Saoud, O., and Bigras, P., 2003, "Conception d'une Loi de Commande Robuste de la Pression Dans un Réservoir Pneumatique á l'aide d'une Formulation IML," *Proceedings of the IEEE Canadian Conference on Electrical Engineering Toward a Caring and Humane Technology*, Montreal, QC, Canada, pp. 001–004.
[34] Khayati, K., Bigras, P., and Dessaint, L.-A., 2004, "A Dynamic Feedback Tracking Design for Systems With Friction Using the LMI Formulation," *Proceedings of the IEEE International Conference on Control Applications*, Vol. 1, pp. 819–824.